Article

Efficient Integration of Fixed-Step Capacitor Banks and D-STATCOMs in Radial and Meshed Distribution Networks Considering Daily Operation Curves

Oscar Danilo Montoya [1,*], Walter Gil-González [2] and Jesus C. Hernández [3,*]

1 Grupo de Compatibilidad e Interferencia Electromagnética (GCEM), Facultad de Ingeniería, Universidad Distrital Francisco José de Caldas, Bogotá 110231, Colombia
2 Department of Electrical Engineering, Universidad Tecnológica de Pereira, Pereira 660003, Colombia; wjgil@utp.edu.co
3 Department of Electrical Engineering, University of Jaén, Campus Lagunillas s/n, Edificio A3, 23071 Jaén, Spain
* Correspondence: odmontoyag@udistrital.edu.co (O.D.M.); jcasa@ujaen.es (J.C.H.)

Abstract: The problem regarding the optimal integration of efficient reactive power compensation in radial and meshed distribution networks using fixed-step capacitor banks and distribution static compensators (D-STATCOMs) is addressed in this research paper by proposing a master–slave optimization methodology. Radial and meshed distribution topologies are considered for the grid structure while including variable active and reactive demand curves. An economic analysis is performed, considering the net present value of the optimization plan, as well as the costs of energy losses and the capacitor banks' acquisition, installation, and operation. In the case of the D-STATCOMs, an annualized costs analysis is presented. In the master stage, the discrete version of the generalized normal distribution optimization (GNDO) algorithm selects the nodes and the sizes of the capacitor banks. In the slave stage, the successive approximations power flow approach is implemented. Numerical results in the IEEE 33-bus grid (with both radial and meshed topologies) and the IEEE 85-bus grid (with a radial configuration) demonstrated the proposed master–slave optimization's effectiveness in minimizing the project's expected net present value for a planning period of five years. Moreover, a simulation in the IEEE 69-bus grid under peak operation conditions showed that the GNDO approach is an excellent optimization technique to solve the studied problem when compared to combinatorial and exact optimization methods. In addition, numerical validations considering D-STATCOMs in the IEEE 85-bus grid confirmed the effectiveness and robustness of the GNDO approach in addressing problems associated with optimal reactive power compensation in medium-voltage distribution systems.

Keywords: fixed-step capacitor banks; net present value optimization; distribution static compensators; daily operative curves; master–slave optimization method; generalized normal distribution optimizer

1. Introduction

The issue of improving the performance of distribution networks has attracted a lot of attention, from researchers to distribution network operators. This improvement implies an adequate management of the devices involved, such as load tap changing at the substation transformer and switched shunt compensators to regulate the voltage profiles and support reactive power. These approaches aim to enhance the operating conditions of distribution networks, e.g., reducing the energy losses costs [1–3]. Furthermore, this improvement can also include upgrading the networks by installing new devices, such as fixed-step capacitor banks and distribution static compensators (D-STATCOMs) [2,4,5]. One of the cheapest ways to compensate for reactive power in distribution grids is through the installation of

fixed-step capacitor banks, which allows for reducing costs due to energy losses by around 13% [4,6].

Fixed-step capacitor banks and D-STATCOMs must be appropriately located in distribution networks, preventing an inadequate operation of the network (i.e., an increase in power losses). An adequate size must also be selected so as to not generate overvoltage (or a voltage decrease) [7]. Thus, the problem regarding the optimal location and sizing of fixed-step capacitor banks in distribution grids has been widely analyzed in the scientific literature. Some of these analyses are presented below.

In specialized literature, the optimal location and sizing of fixed-step capacitor banks in distribution systems has been widely addressed using classical mathematical models and metaheuristic strategies. Combinatorial algorithms such as a discrete version of the vortex search algorithm [7], fuzzy logic [8], the whale optimization algorithm [2], genetic algorithms [9,10], artificial neural networks [11], the spring search algorithm [12], simulated annealing [11], and the particle swarm optimization algorithm [13,14] have been proposed for solving this problem. In Ref. [15], a genetic algorithm combined with mathematical optimization was used to optimally locate and size fixed-step capacitor banks in distribution networks. The objective function involved minimizing the power losses and operating costs of the network. In Ref. [16], a heuristic methodology for the optimal sizing and placement of capacitor banks was proposed. This work considered the reduction of the total harmonic distortion, demonstrating that this methodology could minimize network costs to a greater extent than classical genetic algorithms. Other works have focused on improving voltage stability and, simultaneously, reducing the network power losses, as shown in [17,18]. The authors of [19] included a reconfiguration of distribution networks for the optimal allocation of capacitor banks via a fuzzy-based strategy. The study by [20] considered balanced and unbalanced distribution grids, as well as network reconfiguration and the optimal location of capacitor banks. The authors reduced total active power losses and bus voltage violation indices by employing a hybrid Big Bang-Big Crunch algorithm. The research by [21] presented a hybrid mathematical formulation for the optimal selection and placement of fixed-step capacitor banks in electrical distribution networks, focusing on minimizing the annual operating costs. The authors of [22] transformed the mixed-integer non-convex nonlinear model for the problem under study into a mixed-integer convex one using second-order cone relaxations. Numerical results demonstrated that the convex model found a better solution than the General Algebraic Modeling System (GAMS) software and the Chu and Beasley genetic algorithm.

Multi-objective formulations for the optimal location and sizing of fixed-step capacitor banks have also been proposed, which have usually implemented the Pareto front strategy. This method solves the problem using a set of trade-off solutions, and is known as the Pareto optimality of solutions. The main works in this regard are a multi-objective adaptive algorithm based on decomposition and differential evolution [23], a multi-objective formulation busing a two-stage immune algorithm [24], a hybrid configuration using weight-improved particle swarm optimization and the gravitational search algorithm [25], a multi-objective salp swarm optimizer [26], and multi-objective particle swarm optimization [1], among others. However, these works focus on optimizing technical and economic objectives for a short period of time and do not include the costs of the fixed-step capacitor banks, i.e., regarding their acquisition, operation, and maintenance, along with their useful life.

Similarly, the problem of the optimal location and sizing of D-STATCOMs in distribution systems has been widely studied. The authors of [27] used an artificial rabbits' optimization algorithm for the optimal allocation of PV systems plus D-STATCOM in order to reduce the voltage regulation profile and the energy losses during the day, considering a load curve of 24 h. Similarly to previous authors, the researchers in [28] allocated PV systems plus D-STATCOM in distribution systems to minimize their energy losses and improve their voltage profile using hunter-prey-based algorithm. The authors of [29] located and dimensioned the D-STATCOMs optimally in the electrical distribution grids to

minimize their operative costs based on a discrete-continuous version of the vortex search algorithm. The authors of [30] used a discrete-continuous version of the genetic algorithm in order to locate-size of the D-STATCOM in radial and meshed distribution networks for minimizing their annual operative costs. These costs involved energy losses and installation investment costs annually. The study by [5] tackled sizing and locating D-STATCOMs optimally in electrical distribution networks and implemented a stochastic mixed-integer convex model. This model was performed in a complex domain and included the stochastic nature of renewable energy and demand via multiple scenarios, defining different levels of generation/demand. Although all the previous works can find good solutions, none have considered the expected return rate of the distribution company, as well as the anticipated interest of the increase in energy losses costs in their objective functions. Therefore, in light of the state of the art, this research presents the following contributions:

i.   A general formulation of the problem regarding the optimal placement and sizing of fixed-step capacitor banks and D-STATCOM while considering a planning period different from one year, which includes the expected return rate of the distribution company, the anticipated interest of the increase in energy losses costs, and the increase in the operating expenses of the fixed-step capacitor banks. These aspects are formulated using the net present value as an objective function subjected to a set of mixed-integer nonlinear constraints, thus generating a general mixed-integer nonlinear programming (MINLP) model to represent the studied problem.

ii. The application of the generalized normal distribution optimizer (GNDO) approach and the successive approximations power flow method within master–slave strategy to solve the proposed MINLP model, with the main advantage that different sets of candidate nodes are explored to identify the best solution regarding the final net present value. These simulations found that, as expected, an excessive injection of reactive power is not always adequate in distribution networks. Numerical results confirmed that the radial grid configuration of the IEEE 33-bus grid with two packs of capacitors reached the lowest objective function value. In contrast, for the meshed configuration, only one set of capacitor banks was enough to find the lowest value.

Within the scope of this research, it is worth mentioning that the expected active and reactive power consumptions correspond to the information provided by the distribution company for the terminals of the grid substation, which was obtained after multiple measuring and filtering processes. In addition, the selected objective function is the summation of the purchasing, installing, and operating costs of fixed-step capacitor banks and the annual costs of energy losses, using a net present value analysis for a planning horizon of five years, given that all of the required investments regarding capacitor banks are not recovered with a traditional one-year planning scenario [31].

Note that, in order to validate the effectiveness and robustness of the proposed GNDO approach in locating shunt reactive power compensators, additional simulation scenarios included the peak operating conditions of the IEEE 69-bus grid, the optimal placement and sizing of static distribution compensators in the IEEE 33- and 69-bus grids, and the optimal selection and location of fixed-step capacitor banks in the IEEE 85-bus grid with a radial configuration. These simulations include comparisons with combinatorial optimization methods available in the current literature and the exact MINLP tools of the GAMS software.

This study is organized as follows. Section 2 presents the exact formulation of the optimal location and sizing of fixed-step capacitor banks in electrical distribution networks. Section 3 presents the proposed master–slave optimization model. Section 4 describes the radial and meshed test systems implemented, along with their daily operation curves. Section 5 shows the proposed optimizer model's primary results and analysis. Finally, the main conclusions of this research, as well as some future works, are presented in Section 6.

2. Exact Mathematical Modeling

The efficient integration of fixed-step capacitor banks can be expressed as a mixed-integer nonlinear programming (MINLP) model belonging to the family of mixed-integer non-convex optimization methods. The decision variables regarding the nodal location and size of the fixed-step capacitors are binary. The power flow variables (i.e., power generation, voltages, and currents, among others) are in the real-variable domain. The MINLP model for the efficient reactive power compensation in radial and meshed distribution networks is detailed below.

2.1. Objective Function

The main idea behind integrating fixed-step capacitor banks in distribution grids is to obtain a positive net profit within an expected planning period, i.e., to recover the initial purchasing, installing, and maintenance costs of the capacitor banks, along with an annual reduction in total grid energy losses costs. The objective function for this research corresponds to the net present value (NPV) associated with the energy losses costs for five years, added to the purchasing, installing, and operating costs of the fixed-step capacitor banks. Each one of the objective function's components is presented below.

$$f_1 = C_{kWh} T \left(\sum_{y \in \mathcal{Y}} \left(\frac{1 + i_e}{1 + i_r} \right)^y \right) \left(\sum_{i \in \mathcal{N}} \sum_{j \in \mathcal{N}} \sum_{h \in \mathcal{H}} \left(v_{ih} Y_{ij} v_{jh} \cos \left(\delta_{ih} - \delta_{jh} - \theta_{ij} \right) \Delta_h \right) \right), \quad (1)$$

$$f_2 = \sum_{i \in \mathcal{H}} \sum_{c \in \mathcal{C}} \left(C_c^{\mathrm{purc}} Q_{ic} + C_c^{\mathrm{ins}} + C_c^{\mathrm{ope}} T_c \left(\sum_{y \in \mathcal{Y}} \frac{1 + i_o}{1 + i_r} \right)^y \right) x_{ic}, \quad (2)$$

$$\min f_{\mathrm{NPV}} = f_1 + f_2, \quad (3)$$

where f_1 represents the component of the objective function regarding the net present value of the energy losses costs, and f_2 is the objective function that defines the net present value of the purchasing, installing, and maintenance costs of the reactive power compensators. The sum of both components represents the objective function f_{NPV}. In addition, C_{kWh} is the average cost of the energy losses; T means the number of days in a year; v_{ih} and v_{jh} correspond to the voltage variables at nodes i and j in the period h, which have angles δ_{ih}, and δ_{jh}, respectively; Y_{ij} is the magnitude of the component of the nodal admittance matrix that relates to nodes i and j, which has an angle θ_{ij}; Δ_h is the duration of each load value (daily load variable curve, i.e., typically 1 h); i_e is the interest rate associated with the increase in the energy losses costs; i_o defines the interest rate related to the increase in the operating (maintenance) costs of the fixed-step capacitor banks; i_r corresponds to the expected return rate of the distribution company for each investment; C_c^{purc} defines the purchasing costs of a type-c fixed-step capacitor bank per unit of reactive power injection; C_c^{ins} is a fixed cost associated with the installation of a type-c capacitor bank unit in a particular node of the network; and C_c^{ope} defines the operating/maintenance costs associated with the type-c capacitor bank. The decision variable that establishes whether a type-c fixed-step capacitor bank should be installed at node i is x_{ic}, and T_c is an integer parameter for the type of fixed-step capacitor bank to be used. Note that $\mathcal{N}$ defines the set that contains all the nodes of the network, $\mathcal{Y}$ is the set with the number of years of the planning period, $\mathcal{C}$ is the set containing all of the available fixed-step capacitor bank types, and $\mathcal{H}$ contains all the periods in day of operation.

Remark 1. *The component of the objective function regarding the expected costs of the energy losses, i.e., the component f_1 defined in (1), is a nonlinear non-convex function due to the presence of the product between voltages and trigonometric functions [32]. In contrast, the component f_2 defined in (2) is part of the mixed-integer convex functions due to its linear structure.*

2.2. Set of Constraints

The problem regarding the optimal integration of shunt devices in single-phase distribution networks requires that some technical operative constraints be satisfied. These include active and reactive power balance, voltage regulation limits, and the number of shunt devices. The complete set of constraints is listed below.

$$p_{ih}^g - p_{ih}^d = v_{ih} \sum_{j \in \mathcal{N}} Y_{ij} v_{jh} \cos\left(\delta_{ih} - \delta_{jh} - \theta_{ij}\right), \ \{\forall h \in \mathcal{H}, \ \forall i \in \mathcal{N}\} \tag{4}$$

$$q_{ih}^g - p_{ih}^d + \sum_{c \in \mathcal{C}} Q_{ic} x_{ic} = v_{ih} \sum_{j \in \mathcal{N}} Y_{ij} v_{jh} \sin\left(\delta_{ih} - \delta_{jh} - \theta_{ij}\right), \ \{\forall h \in \mathcal{H}, \ \forall i \in \mathcal{N}\} \tag{5}$$

$$p_i^{g,\min} \leq p_{ih}^g \leq p_i^{g,max}, \ \{\forall h \in \mathcal{H}, \ \forall i \in \mathcal{N}\} \tag{6}$$

$$q_i^{g,\min} \leq q_{ih}^g \leq q_i^{g,max}, \ \{\forall h \in \mathcal{H}, \ \forall i \in \mathcal{N}\} \tag{7}$$

$$v_{\min} \leq v_{ih} \leq v_{\max}, \ \{\forall h \in \mathcal{H}, \ \forall i \in \mathcal{N}\} \tag{8}$$

$$\sum_{c \in \mathcal{C}} \sum_{i \in \mathcal{N}} x_{ic} \leq N_{cap}^{ava}, \tag{9}$$

$$\sum_{c \in \mathcal{C}} x_{ic} \leq 1, \{\forall i \in \mathcal{N}\} \tag{10}$$

$$x_{ic} \in \{0,1\}, \ \{\forall c \in \mathcal{C}, \ \forall i \in \mathcal{N}\} \tag{11}$$

where p_{ih}^g and q_{ih}^g are the active and reactive power generation outputs of a power source connected at node i in each period; p_{ih}^d and q_{ih}^d represent the active and reactive power consumption (constant power loads) at each node and in each period; $p_i^{g,\min}$ and $p_i^{g,max}$ correspond to the lower and upper active power generation bounds assigned to the power source connected at node i; $q_i^{g,\min}$ and $q_i^{g,max}$ correspond the lower and upper reactive power generation bounds assigned to the power source connected at node i; $v_{\min}$ and $v_{\max}$ are the minimum and maximum values assigned for the voltage variable at each node; and N_{cap}^{ava} is the number of capacitor banks available for installation.

Note that the set of constraints (4)–(11) can be understood as follows. Equations (4) and (5) are the active and reactive power balance equilibrium per node and period [33]. Inequality constraints (6) and (7) define the lower and upper bounds of the generation variables associated with the power sources connected at node i in any period. Box-type constraint (8) defines the well-known voltage regulation constraint applicable to medium-voltage distribution grids by regulatory commissions in each country [34]. Inequality constraint (9) defines the number of fixed-step capacitor banks available for installation in the entire distribution network. In contrast, inequality constraint (10) allows having a maximum of one type of fixed-step capacitor bank per node. Finally, (11) confirms the binary nature of the decision variable regarding the location or not of a set of fixed-step capacitor banks in a particular node of the network.

Remark 2. *The set of constraints (4)–(11) defines a mixed-integer non-convex solution space due to nonlinear constraints regarding the active and reactive power balance per node and period described in (4) and (5) [35].*

To solve the proposed optimization models (1)–(11), the current literature recommends the application of master–slave optimization methods based on hybrid formulations [20]. These use combinatorial optimizers for the integer (binary) part of the optimization model, and power flow methods for solving the continuous part [21]. The following section details the application of the proposed GNDO approach.

3. Proposed Master–Slave Optimizer

A master–slave optimization methodology is proposed to deal with the problem regarding the efficient integration of fixed-step capacitor banks in distribution grids with

radial and meshed configurations. The master stage defines the set of binary variables (i.e., the values of x_{ic}) per node and capacitor type. The slave stage solves the power flow problem while considering the insertion of the capacitor banks provided by the master stage. It is worth mentioning that, in the proposed strategy, the master stage corresponds to the GNDO approach using a discrete codification, and the slave stage involves the successive approximations method. In addition, note that,

i. with the master stage using a discrete codification, it is possible to obtain the value of the f_2 component of the objective function, i.e., the purchasing, installation, and maintenance costs of the fixed-step capacitor banks;

ii the slave stage determines the expected energy losses costs of the network for the planning period, as these depend on the expected demand behavior and the values regarding the active and reactive power consumption per node.

The main characteristics of the master and slave components of the proposed solution methodology are detailed below.

3.1. Slave Stage: Successive Approximations Power Flow Approach

In the current literature, multiple specialized power flow algorithms have been reported for addressing the nonlinearities in Equations (4) and (6) via numerical methods [36]. An efficient power flow method for radial and meshed distribution networks has been proposed in the literature [37]. This approach is a generalization of the classical backward/forward power flow method using nodal admittance matrices, which was named *the successive approximations method* due to its similarities with the classical Gauss–Seidel power flow approach. The successive approximations power flow method belongs to the family of derivative-free power flow methods, implying that its convergence is linear. On the other hand, derivative-based power flow methods converge quadratically, as is the case of the Newton–Raphson approach [38]. The successive approximations method is efficient regarding processing times, as only one inverse matrix is used during all solution processes. This is not true for derivative-based approaches [39].

The iterative power flow formula for solving Equations (4) and (6) is defined in the complex domain as shown in (12).

$$\mathbb{V}_{dh}^{m+1} = -\mathbf{Y}_{dd}^{-1}\left(\mathbf{diag}^{-1}\left(\mathbb{V}_{dh}^{m,\star}\right)\left(\mathbb{S}_{dh}^{\star} - \mathbb{S}_{ch}^{\star}\right) + \mathbf{Y}_{dg}\mathbb{V}_{gh}\right), \{\forall h \in \mathcal{H}\} \tag{12}$$

where m is the iterative counter, $\mathbb{V}_{dh}$ is a complex vector containing the voltage variables in all of the demand nodes per period; $\mathbb{V}_{gh}$ corresponds to a vector that contains the voltage values in the slack source; $\mathbf{Y}_{dd}$ is a square matrix associated with the admittance relations between demand nodes; $\mathbf{Y}_{dg}$ is a rectangular matrix that contains the complex relations between the demand and slack nodes; $\mathbb{S}_{dh}$ is a vector containing the set of constant demand power loads per node and period; and $\mathbb{S}_{ch}$ corresponds to the vector of complex power injections in the selected nodes where capacitors must be placed. Note that $\mathbb{X}^{\star}$ denotes the application of the conjugate operator to the complex vector $\mathbb{X}$.

Remark 3. *Note that the vector $\mathbb{S}_{ch}$ contains the variables that relate the master stage to the slave stage, as the master stage defines the set of nodes and capacitor sizes. This is fixed in the slave stage to solve the power flow problem with the recursive formula (12).*

The convergence criterion applied to the power flow formula in (12), as recommended by the authors of [37], is the error between two consecutive voltage iterations, i.e.,

$$\max_{h \in \mathcal{H}}\left\{\left\|\left|\mathbb{V}_{dh}^{m+1}\right| - \left|\mathbb{V}_{dh}^{m}\right|\right\|\right\} \leq \varrho, \tag{13}$$

where $\mathbb{V}_{dh}^0$ corresponds to the vector with the initial voltage values, which are set as equal to the voltage at the substation bus (i.e., $\mathbb{V}_{gh}$). In addition, ϱ is the maximum tolerance error, set as 1×10^{-10} [39].

Once the power flow formula (12) has reached the desired convergence in (13), the expected grid power losses can be calculated as follows:

$$f_1 = C_{kWh} T \left(\sum_{y \in \mathcal{Y}} \left(\frac{1 + i_e}{1 + i_r} \right)^y \right) \sum_{h \in \mathcal{H}} \mathbb{V}_h^\top (\mathbf{Y}^\star \mathbb{V}_h), \tag{14}$$

where $\mathbb{V}_h$ is the vector containing the voltage profiles of the distribution network, including the slack source per period (i.e., $\mathbb{V}_h = \left[\mathbb{V}_{gh} \; \mathbb{V}_{dh} \right]^\top$), and $\mathbf{Y}$ is the nodal admittance matrix of the distribution network under analysis.

3.2. Master Stage: The Generalized Normal Distribution Optimizer (GNDO)

The GNDO approach is a recently developed combinatorial optimization method inspired by the statistical properties of a Gaussian distribution. It was originally proposed by the authors of [40] to solve the problem regarding the parametric estimation of photovoltaic modules. The main advantage of the GNDO approach is that its exploration and exploitation rules do not require any special adjustment parameter. It begins the exploration of the solution space with a random population that evolves with simple rules [41]. The general structure of a Gaussian distribution is defined in (15).

$$f(x) = \frac{1}{\sqrt{2\pi}\delta} \exp\left(\frac{(x - \mu)^2}{2\delta^2} \right), \tag{15}$$

where x is a set of variables associated with the distribution probability, which is randomly generated. These variables are defined by the location parameter μ and the scaling parameter δ [41]. From Equation (15), it can be noted that the parameters δ and μ are the key factors in the generation of the Gaussian distribution, the former being associated with the standard deviation and the latter with the mean value, respectively [40].

Remark 4. *Note that the Gaussian distribution formula in (15) allows defining the initial population, i.e., the set of initial solutions, which takes the following form:*

$$x_k^t = \left[5, i, \dots, 15 \mid 1, c, \dots, 6 \right], \tag{16}$$

where the dimension of x_k^t is a $1 \times N_{cap}^{ava}$, corresponding to a discrete representation of the x_{ic}. In the potential solution presented in (16), it is observed that a type-1 capacitor is located at node 5, a type-c one at node i, and a type-6 one at node 15. In addition, k denotes the position of the solution individual in the population composed of N_s vectors, as in (16).

It is worth mentioning that, with the codification presented in (16), the second component of the objective function f_2 is obtained, i.e., the purchasing, installation, and operating costs of the fixed-step capacitor banks, which, for example, in (16), implies that $x_{5,1}$, x_{ic}, and $x_{15,6}$ are activated. The remainder of binary variables is maintained at zero.

Considering the general codification of a potential solution to the studied problem, the local and global searches through the solution space with the GNDO approach are detailed below.

3.2.1. Local Search Characteristic: Exploitation of the Solution Space

In this stage, the GNDO approach intensifies its exploration in a local area around the best current solution found in order to accelerate its speed of convergence [42]. The general evolution formula for this local exploration is defined in (16).

$$v_k^t = \mu_k + \eta \delta_k, \ k = 1, 2, \ldots, N_s. \tag{17}$$

where η is defined as a penalty factor; δ_k corresponds to the generalized standard variation; μ_k means the generalized mean position; and v_k^t is a potential solution individual. Each of the terms in (17) is calculated as follows:

$$\mu_k = \frac{1}{3} \left(x_k^t + x_{\text{best}}^t + U \right), \tag{18}$$

$$\delta_k = \frac{1}{\sqrt{3}} \left(\left(x_k^t - \mu_k \right)^2 + \left(x_{\text{best}}^t - \mu_k \right)^2 + (U - \mu_k)^2 \right)^{\frac{1}{2}} \right), \tag{19}$$

$$\eta = \begin{cases} \sqrt{(-\log(\lambda_1))} \cos(2\pi\lambda_2), & if \ a \leq b \\ \sqrt{(-\log(\lambda_1))} \cos(2\pi\lambda_2 + \pi), & if \ a > b \end{cases} \tag{20}$$

where a, b, λ_1, and λ_2 are randomly generated in the interval $[0, 1]$ with a uniform distribution; x_{best}^t represents the best solution reached until iteration t; and U is a vector associated with the average position of all the individuals in the current population at iteration t.

$$U = \frac{1}{N_s} \sum_{k=1}^{N_s} x_k^t, \tag{21}$$

Remark 5. *Once the potential solution v_k^t is generated using Equations (18) to (20), as presented in (17), a feasibility check is implemented. This implies that*

$$v_{kl}^t = \begin{cases} v_{kl}^t, & if \ x_l^{\min} \leq v_{kl}^t \leq x_l^{\max} \\ round\left(x_l^{\min} + r\left(x_l^{\min} - x_l^{\min}\right)\right) & Otherwise \end{cases}, \tag{22}$$

where $x_l^{\max}$ and $x_l^{\min}$ are the minimum and maximum limits allowed for the decision variable in the lth position.

3.2.2. Global Search Characteristic: Exploration of the Solution Space

The main idea behind using a global exploration characteristic for combinatorial optimization methods is the possibility of allowing them to escape from locally optimal solutions by exploring new regions of the solution space [43]. The general formula to implement global exploration in the GNDO approach is defined below [40].

$$v_k^t = x_k^t + \beta(|\lambda_3|v_1) + (1 - \beta) * (|\lambda_4|v_2), \tag{23}$$

where λ_3 and λ_4 are two randomly generated numbers between 0 and 1 that are subject to a normal distribution, and β is a calling and adjustment parameter generated between 0 and 1 with a uniform distribution. In addition, v_1 and v_2 are two trail vectors calculated as defined in (24) and (25).

$$v_1 = \begin{cases} x_k^t - x_j^t, & if \ F_f\left(x_k^t\right) < F_f\left(x_j^t\right) \\ x_j^t - x_k^t, & Otherwise \end{cases}, \tag{24}$$

$$v_2 = \begin{cases} x_i^t - x_m^t, & if \ F_f\left(x_i^t\right) < F_f\left(x_m^t\right) \\ x_m^t - x_i^t, & Otherwise \end{cases}, \tag{25}$$

where the values of positions i, j, and m are randomly generated between 1 and the number of potential solutions (i.e., N_s), with the main characteristic that all of them must be different

from each other and the current solution located at position k. In addition, $F_f\left(x_k^t\right)$ defines the value of the fitness function, considered as an adaptive representation of the objective function [41]. Note that, in order to maintain the feasibility of the solution space regarding the minimum and maximum permitted values for the decision variables, the revision formula (22) is applied to the potential solution v_k^t in (23).

Finally, the following evolution rule is applied to ensure that the best solution for the current population will be maintained:

$$x_k^{t+1} = \begin{cases} v_k^t, & if\ F_f(v_k^t) \leq\ F_f(x_k^t) \\ x_k^t, & \text{Otherwise} \end{cases}. \tag{26}$$

3.2.3. General Implementation of the Master–Slave Optimization Approach

To illustrate the general implementation of the solution approach, a flow diagram is presented in Figure 1.
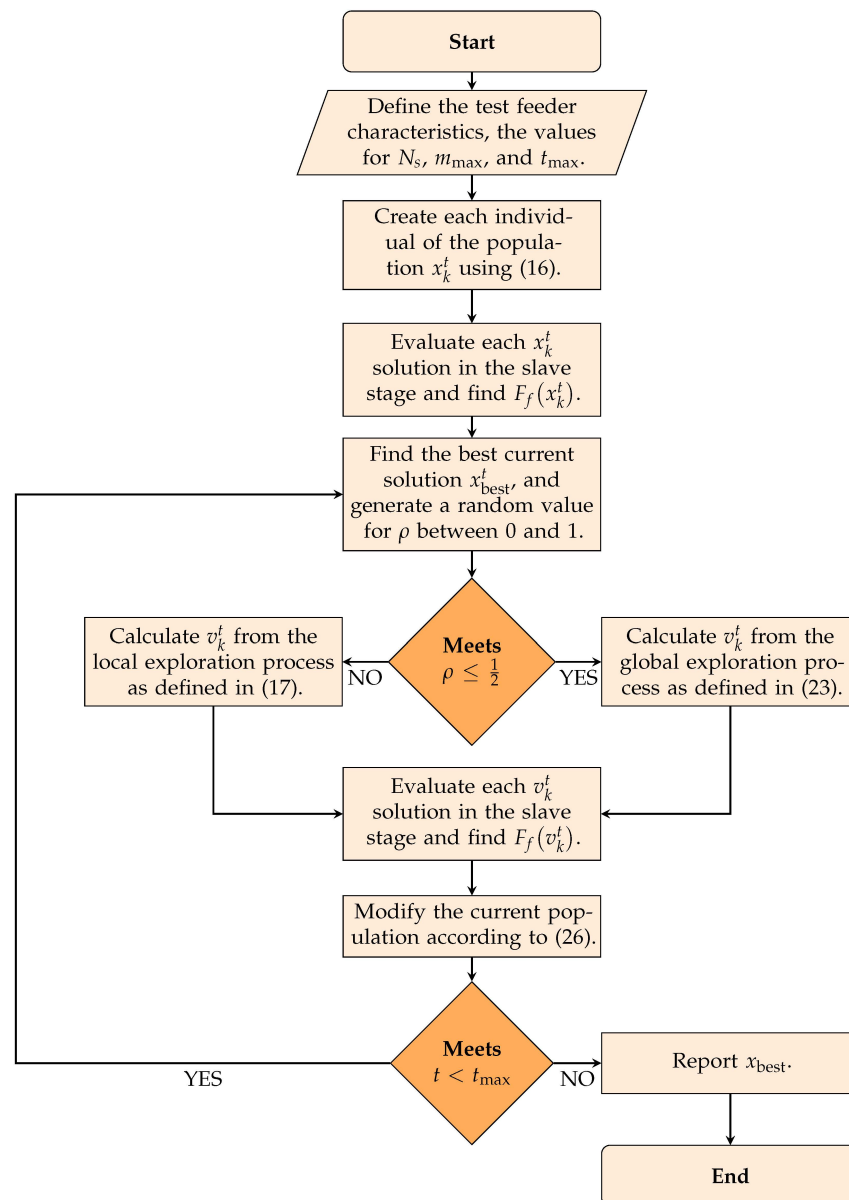
Figure 1. Flowchart for the improved GNDO.

Remark 6. *The main characteristic in Figure 1 is the intrinsic relationship between the master and slave stages, as each v_k^t generated with the GNDO approach requires evaluation by the power flow problem to determine the total costs of the power losses using the slave stage [44].*

4. Test Feeder Characterization

To validate the proposed GNDO approach in combination with the successive approximations power flow method to locate and size fixed-step capacitor banks while aiming to reduce the expected annual operating costs associated with energy losses and including the purchasing, installing, and operating costs of reactive power compensators, the IEEE 33-bus grid with radial and meshed configurations was employed. Figure 2 depicts the electrical configurations of this test feeder.
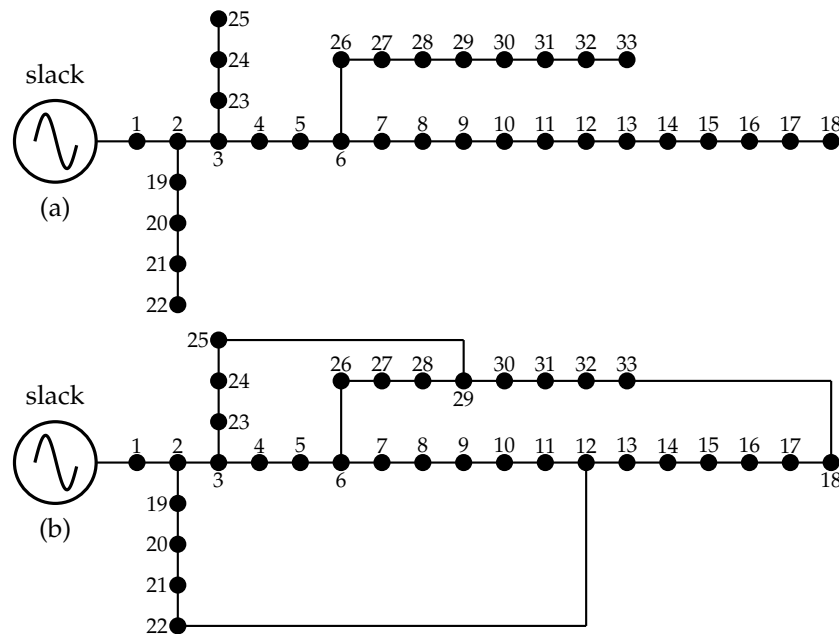
Figure 2. Single line diagrams for the IEEE 33-bus grid: (**a**) radial and (**b**) meshed configurations.

Data regarding branches and peak load conditions for the IEEE 33-bus grid are presented in Table 1.

In addition, to evaluate the effect of load variations, Figure 3 presents the daily variations regarding the active and reactive power profiles.
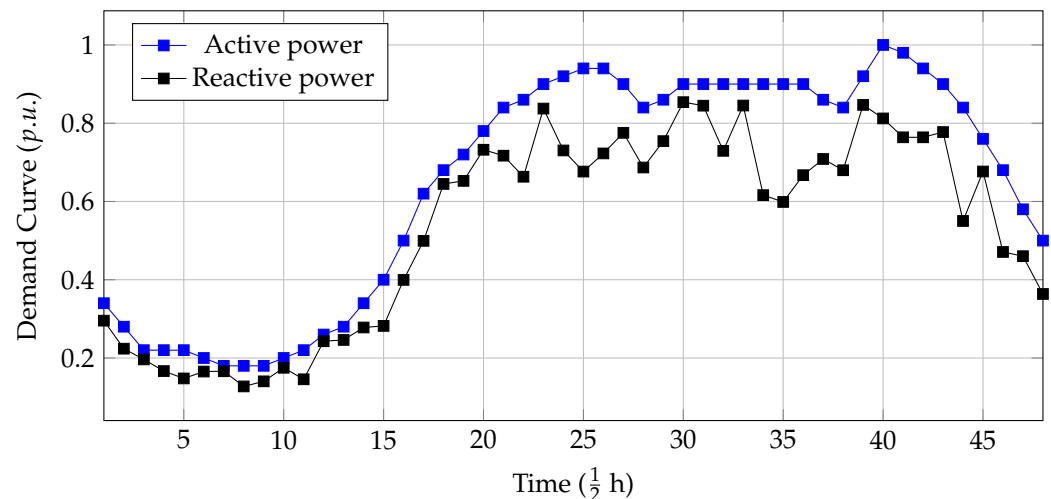
Figure 3. Daily variations for loads considering active and reactive power curves.

Table 1. Parametric information of the IEEE 33-bus grid with radial and meshed configurations.

Bus i	Bus j	R_{ij} (Ω)	X_{ij} (Ω)	P_j (kW)	Q_j (kvar)
1	2	0.0922	0.0477	100	60
2	3	0.4930	0.2511	90	40
3	4	0.3660	0.1864	120	80
4	5	0.3811	0.1941	60	30
5	6	0.8190	0.7070	60	20
6	7	0.1872	0.6188	200	100
7	8	1.7114	1.2351	200	100
8	9	1.0300	0.7400	60	20
9	10	1.0400	0.7400	60	20
10	11	0.1966	0.0650	45	30
11	12	0.3744	0.1238	60	35
12	13	1.4680	1.1550	60	35
13	14	0.5416	0.7129	120	80
14	15	0.5910	0.5260	60	10
15	16	0.7463	0.5450	60	20
16	17	1.2890	1.7210	60	20
17	18	0.7320	0.5740	90	40
2	19	0.1640	0.1565	90	40
19	20	1.5042	1.3554	90	40
20	21	0.4095	0.4784	90	40
21	22	0.7089	0.9373	90	40
3	23	0.4512	0.3083	90	50
23	24	0.8980	0.7091	420	200
24	25	0.8960	0.7011	420	200
6	26	0.2030	0.1034	60	25
26	27	0.2842	0.1447	60	25
27	28	1.0590	0.9337	60	20
28	29	0.8042	0.7006	120	70
29	30	0.5075	0.2585	200	600
30	31	0.9744	0.9630	150	70
31	32	0.3105	0.3619	210	100
32	33	0.3410	0.5302	60	40
12	22	2	2	-	-
18	33	0.5	0.5	-	-
25	29	0.5	0.5	-	-

To evaluate the objective function regarding expected energy losses costs during the planning period, as well as the purchasing, installation, and operating costs of the fixed-step capacitor banks, the parameters listed in Table 2 are considered.

Table 2. Parametric information to evaluate the objective function.

Parameter	Value	Unit	Parameter	Value	Unit
C_{kWh}	0.1390	USD-kW/h	T	365	days
Δ_h	0.5	h	i_e	8	%
i_r	15	%	i_o	10	%
$|\mathcal{Y}|$	5	Year	C_c^{purc}	25	USD/kvar
C_c^{ins}	1600	USD	C_c^{ope}	300	USD/bank-year

Note that the step-size per capacitor is 100 kvar, and the maximum reactive power injection per node is 1000 kvar, i.e., from 0 to 10 banks in parallel per node.

5. Numerical Results

For the computational implementation of the proposed master–slave optimization approach, the MATLAB software (version 2021b) was employed on a PC with an AMD Ryzen 7 3700 2.3 GHz processor and 16.0 GB RAM, running a 64-bit version of Microsoft

Windows 10 Single Language. The GNDO and the successive approximations power flow method were implemented with our developed scripts. For the simulations, the possibility of installing 0 to 5 sets of capacitor banks is tested by assuming that only a pack can be installed per node.

Note that the parametrization of the GNDO approach considered a population size of 10 individuals, 100 consecutive repetitions, and 1000 iterations, with a local stopper of 100 iterations without improvements in the objective function value.

5.1. Results Obtained for the Radial Grid Configuration

Table 3 presents the numerical simulations for the IEEE 33-bus grid with a radial topology. In this simulation, each node selected to locate a reactive power compensator must have at least one pack of capacitors installed.

Table 3. Numerical results for the IEEE 33-bus grid with a radial topology.

No. of Nodes	Location	Size (kvar)	f_{NPV} (USD)	Ave. Time (s)
0	-	-	468,749.2023	-
1	30	600	410,939.1048	62.9109
2	[13, 30]	[200, 500]	403,811.3704	68.8260
3	[11, 15, 30]	[100, 100, 500]	404,805.4441	49.9192
4	[11, 15, 30, 32]	[100, 100, 400, 100]	405,860.1101	51.5080
5	[11, 14, 29 30, 31]	[100, 100, 100 200, 200]	407,754.4498	45.8391

The numerical results in Table 3 show that:

i.   An increase in the number of capacitors does not guarantee that the objective function will continue to decrease; for the radial version of the IEEE 33-bus grid with the available set of capacitors (steps of about 100 kvar), it is observed that the option with two capacitors at nodes 13 and 30 with sizes of about 200 and 500 kvar allows for the best reduction concerning the benchmark case (i.e., 13.8534%). In contrast, all the other options report lower impacts in the final objective function value.

ii. Note that from three to five sets of capacitor banks, the objective function deteriorates with the increase in capacitors, which confirms that, depending on the electrical characteristics (i.e., grid topology and total active and reactive power consumptions), each distribution network has an optimal number regarding compensation devices, and, if this number is exceeded, the final solution becomes sub-optimal. Note that the expected improvement in the objective function is 13.0122% when five capacitors are installed, showing that the expected gain has deteriorated about 0.8412% concerning the best solution reported in Table 3.

iii. The main characteristic of the list of solutions in Table 3 is that the most interesting node to install capacitor banks is node 30, which appears in all of the solutions, with sizes between 400 and 600 kvar (thus being the node with the highest penetration regarding reactive power in all solutions). In addition, the expected penetration regarding reactive power varies from 600 to 700 kvar.

Regarding processing times, it is worth mentioning that the last column in Table 3 evidences that the processing times required for solving the MINLP model via the proposed GNDO approach range between 45 and 69 s to reach a solution, depending on the number of nodes analyzed. However, it is noted that these times can be considered minimal due to the enormous dimensions of the solution space for this optimization problem.

5.2. Results Obtained for the Meshed Grid Configuration

Table 4 presents the numerical simulations for the IEEE 33-bus grid with a meshed topology.

Table 4. Numerical results for the IEEE 33-bus grid with meshed topology.

No. of Nodes	Location	Size (kvar)	f_{NPV} (USD)	Ave. Time (s)
0	-	-	302,404.0994	-
1	30	600	279,154.9647	42.2342
2	[30, 32]	[400, 200]	279,488.0998	42.2345
3	[14, 30, 32]	[100, 400, 100]	280,597.3739	47.9757
4	[16, 29, 30, 32]	[100, 100, 300, 100]	282,273.7510	46.2040
5	[8, 13, 25 30, 31]	[100, 100, 100 300, 100]	284,287.0318	40.7188

The numerical results in Table 4 show that:

i. In the case of the meshed version of the IEEE 33-bus grid, the best solution is reached by only installing a capacitor bank of 600 kvar at node 30, which allows for a reduction of about 7.6881% concerning the benchmark case. However, this solution is very closely followed by the solution with two capacitor banks at nodes 30 and 32, with sizes of 400 and 200 kvar, which allows for a reduction of about 7.5779% with respect to the benchmark case, i.e., a slight variation of 0.1102% between both solutions.

ii. As in the radial version of the IEEE 33-bus grid, node 30 seems to be the most attractive node to install a set of capacitor banks; in all solutions, this node appears with the highest value of reactive power injection, which implies that, for this test feeder, node 30 is key for optimal reactive power compensation, regardless of the grid topology under analysis.

iii. The difference between the best solution with one pack of capacitors at node 30 and the solution with five capacitors is about USD 5132.0671, which confirms that an increase in the number of fixed-step capacitor banks is not necessarily the most economical solution, since it depends exclusively on the grid topology, the number of nodes, and the demand behavior.

Regarding processing times, it is observed that, on average, the solution times required by the GNDO approach in the meshed configuration are lower than 48 s, and lower than the times taken by the radial topology. However, this is an expected behavior, given that, for meshed grid configurations, the successive approximations power flow method takes fewer iterations in comparison with the radial topology, which finally translates into reduced processing times.

5.3. Complementary Analysis

This subsection presents additional numerical validations to demonstrate the efficiency of the proposed GNDO approach for selecting and installing reactive power compensators in distribution networks. These analyses include the following:

i. Illustrating the energy losses behavior in the IEEE 33-bus grid with radial and meshed configurations.

ii. A comparative analysis of the GNDO approach in the IEEE 69-bus grid with different combinatorial optimizers regarding the optimal selection and location of fixed-step capacitor banks for power losses minimization while considering peak load operating conditions.

iii. A comparative analysis in the radial versions of the IEEE 33-and 69-bus grids considering static distribution compensators (D-STATCOMs) with respect to literature reports.

iv. An evaluation of the proposed master–slave approach in the IEEE 85-node test feeder with zero to five capacitors. These will be considered as new reference results in medium-size distribution networks for future optimization algorithms.

5.3.1. Energy Losses Behavior in the Radial and Meshed Versions of the IEEE 33-bus Grid

To illustrate the positive effect of the optimal integration of fixed-step capacitor banks in radial and meshed distribution networks, Figure 4a,b present the initial daily energy losses without capacitor banks, as well as the best solutions reported in Tables 3 and 4.
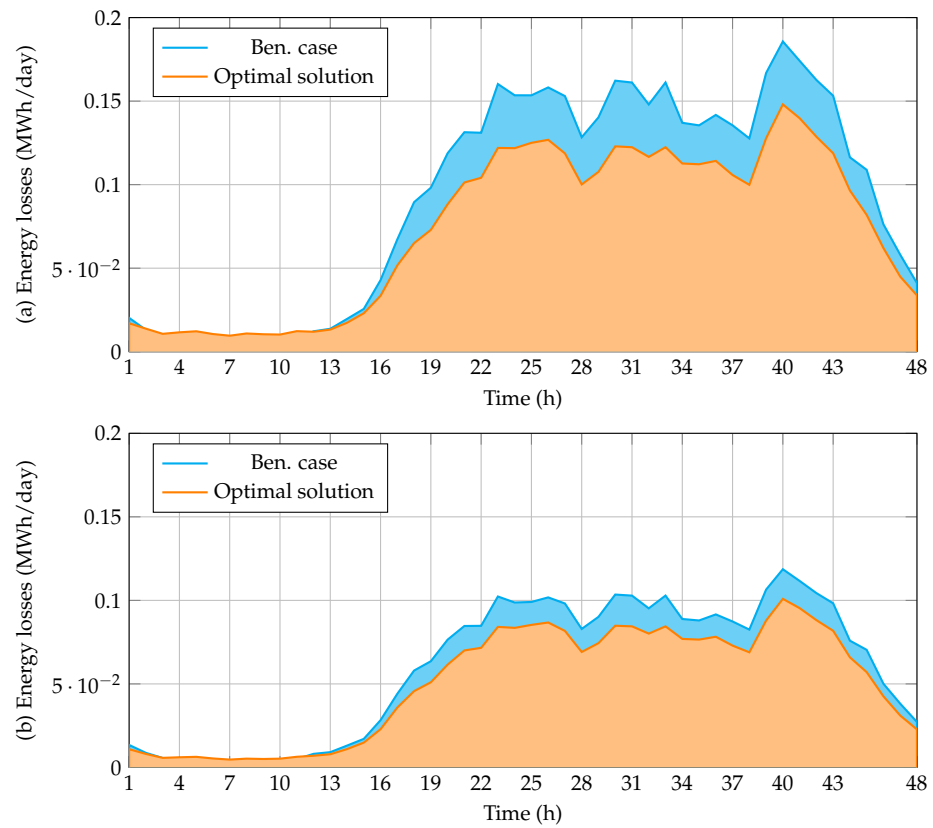
Figure 4. Daily energy losses behavior for the radial and meshed networks when comparing the benchmark case vs. the optimal solution: (**a**) radial and (**b**) meshed configurations.

The main characteristic of the daily energy losses behavior in Figure 4 is that the fixed reactive power injection effectively reduces the total grid power losses throughout the day, as observed in the difference between the benchmark curve and the optimal solution curves.

5.3.2. Optimal Selection and Location of Fixed-Step Capacitor Banks in the IEEE 69-bus Grid

To demonstrate that the proposed GNDO approach is an efficient optimization technique for integrating fixed-step capacitor banks, a comparative analysis with different combinatorial methods and exact optimization method is presented, using the IEEE 69-bus grid as a test feeder. The electrical configuration of this system and its branch load parameters are depicted in Figure 5 and Table 5, respectively.
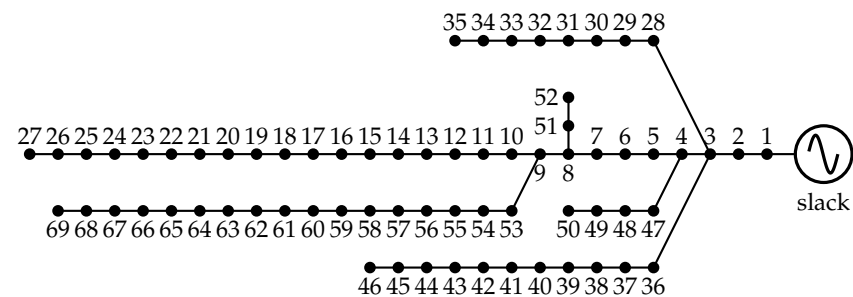
Figure 5. Schematic nodal connections in the IEEE 69-bus grid.

Table 5. Branch and load parameters for the IEEE 69-bus system.

Node i	Node j	R_{ij} (Ω)	X_{ij} (Ω)	P_j (kW)	Q_j (kvar)	Node i	Node j	R_{ij} (Ω)	X_{ij} (Ω)	P_j (kW)	Q_j (kvar)
1	2	0.0005	0.0012	0.00	0.00	3	36	0.0044	0.0108	26.00	18.55
2	3	0.0005	0.0012	0.00	0.00	36	37	0.0640	0.1565	26.00	18.55
3	4	0.0015	0.0036	0.00	0.00	37	38	0.1053	0.1230	0.00	0.00
4	5	0.0251	0.0294	0.00	0.00	38	39	0.0304	0.0355	24.00	17.00
5	6	0.3660	0.1864	2.60	2.20	39	40	0.0018	0.0021	24.00	17.00
6	7	0.3810	0.1941	40.40	30.00	40	41	0.7283	0.8509	1.20	1.00
7	8	0.0922	0.0470	75.00	54.00	41	42	0.3100	0.3623	0.00	0.00
8	9	0.0493	0.0251	30.00	22.00	42	43	0.0410	0.0478	6.00	4.30
9	10	0.8190	0.2707	28.00	19.00	43	44	0.0092	0.0116	0.00	0.00
10	11	0.1872	0.0619	145.00	104.00	44	45	0.1089	0.1373	39.22	26.30
11	12	0.7114	0.2351	145.00	104.00	45	46	0.0009	0.0012	29.22	26.30
12	13	1.0300	0.3400	8.00	5.00	4	47	0.0034	0.0084	0.00	0.00
13	14	1.0440	0.3450	8.00	5.50	47	48	0.0851	0.2083	79.00	56.40
14	15	1.0580	0.3496	0.00	0.00	48	49	0.2898	0.7091	384.70	274.50
15	16	0.1966	0.0650	45.50	30.00	49	50	0.0822	0.2011	384.70	274.50
16	17	0.3744	0.1238	60.00	35.00	8	51	0.0928	0.0473	40.50	28.30
17	18	0.0047	0.0016	60.00	35.00	51	52	0.3319	0.1114	3.60	2.70
18	19	0.3276	0.1083	0.00	0.00	9	53	0.1740	0.0886	4.35	3.50
19	20	0.2106	0.0690	1.00	0.60	53	54	0.2030	0.1034	26.40	19.00
20	21	0.3416	0.1129	114.00	81.00	54	55	0.2842	0.1447	24.00	17.20
21	22	0.0140	0.0046	5.00	3.50	55	56	0.2813	0.1433	0.00	0.00
22	23	0.1591	0.0526	0.00	0.00	56	57	1.5900	0.5337	0.00	0.00
23	24	0.3463	0.1145	28.00	20.00	57	58	0.7837	0.2630	0.00	0.00
24	25	0.7488	0.2475	0.00	0.00	58	59	0.3042	0.1006	100.00	72.00
25	26	0.3089	0.1021	14.00	10.00	59	60	0.3861	0.1172	0.00	0.00
26	27	0.1732	0.0572	14.00	10.00	60	61	0.5075	0.2585	1244.00	888.00
3	28	0.0044	0.0108	26.00	18.60	61	62	0.0974	0.0496	32.00	23.00
28	29	0.0640	0.1565	26.00	18.60	62	63	0.1450	0.0738	0.00	0.00
29	30	0.3978	0.1315	0.00	0.00	63	64	0.7105	0.3619	227.00	162.00
30	31	0.0702	0.0232	0.00	0.00	64	65	1.0410	0.5302	59.00	42.00
31	32	0.3510	0.1160	0.00	0.00	11	66	0.2012	0.0611	18.00	13.00
32	33	0.8390	0.2816	14.00	10.00	66	67	0.0470	0.0140	18.00	13.00
33	34	1.7080	0.5646	19.50	14.00	12	68	0.7394	0.2444	28.00	20.00
34	35	1.4740	0.4873	6.00	4.00	68	69	0.0047	0.0016	28.00	20.00

Table 6 presents all of the numerical comparisons with the IEEE 69-bus grid for locating and sizing fixed-step capacitor banks in radial distribution grids. Note that this comparison is made while considering peak load conditions, as well as with the primary objective of minimizing the expected power losses.

Table 6. Optimal location of fixed-step capacitor banks in the IEEE 69-bus grid.

Method	Nodes	Size [kvar]	Losses [kW]
Base case	-	-	225.072
GSA [45]	{11, 29, 60}	{900, 1050, 450}	163.280
TSM [46]	{19, 62, 63}	{225, 900, 225}	148.910
TBLO [47]	{12, 61, 64}	{600 1050, 150}	146.350
FPA [48]	{11, 61, 22}	{450, 1350 150}	145.860
MI-SOCP [22]	{11, 18, 61}	{300, 300, 1200}	145.397
GNDO	{11, 18, 61}	{300, 300, 1200}	145.397

In Table 6, the metaheuristic algorithms used for comparison are the gravitational search algorithm (GSA) [45], the two-stage method (TSM) [46], the teaching-based learning optimizer (TBLO) [47], and the flower pollination algorithm (FPA) [48], and the convex optimization method corresponds to the mixed-integer second-order cone programming (MI-SOCP) approach [22]. Only the GNDO and the MI-SOCP approaches found the best

possible solution in the IEEE 69-bus grid when power losses were minimized under peak load conditions. Both methods found the same set of nodes (11, 18, and 31), with capacitor sizes of 300 kvar in the first two and 1200 kvar in the last one. Note that the remainder of metaheuristic algorithms are stuck in locally optimal solutions, which can be attributed to the large dimensions of the solution space, confirming that the GNDO approach based on a statistical formulation (Gaussian distributions) is an efficient tool to deal with complex MINLP models; as demonstrated in the previous sections, it is an excellent alternative to locate and size fixed-step capacitor banks in radial and meshed distribution grids.

5.3.3. Optimal Location and Sizing of D-STATCOMs in the IEEE 33- and 69-bus Grids

To confirm the effectiveness and efficiency of the proposed GNDO approach in defining the optimal location and sizing of reactive power compensators in electrical distribution networks, this subsection presents the application of this algorithm to the problem regarding the optimal placement and sizing of D-STATCOMs in the IEEE 33- and 69-bus grids with radial configurations.

For this comparison, the objective function considers the investment costs of D-STATCOMs (z_1) and the operating costs associated with the energy losses (z_2), considering a one-year period of study. Both functions are algebraically summed, as defined by z_{cost}. The structure of the studied objective functions is presented below.

$$z_1 = T\left(\frac{k_1}{k_2}\right) \sum_{k \in \mathcal{N}} \left(\omega_1 \left(q_k^{\text{comp}}\right)^2 + \omega_2 q_k^{\text{comp}} + \omega_3\right) q_k^{\text{comp}}, \tag{27}$$

$$z_2 = C_{kWh} T \sum_{h \in \mathcal{H}} \sum_{k \in \mathcal{N}} \sum_{m \in \mathcal{N}} Y_{km} v_{kh} v_{mh} \cos(\delta_{kh} - \delta_{mh} - \theta_{km}) \Delta h, \tag{28}$$

$$\min\ z_{\text{cost}} = z_1 + z_2, \tag{29}$$

where k_1 and k_2 are positive constant parameters associated with the annualization of the investment costs of the shunt compensators, considering a planning period of 10 years [3] q_k^{comp} is the nominal size of the shunt reactive power compensator located at node k; and ω_1, ω_2, and ω_3 are the cubic, quadratic, and linear coefficients regarding the investment costs in shunt reactive power compensators.

The parameters used for evaluating the objective functions in (27) and (28) are listed in Table 7 [49]. Note that the remaining parameters were previously defined in Table 2.

Table 7. Parametrization of the objective function for evaluating the location of D-STATCOMs in distribution grids.

Par.	Value	Unit	Par.	Value	Unit
k_1	6/2190	1/Days	k_2	10	Years
D-STATCOM					
ω_1	(USD/Mvar^3)	ω_2	(USD/Mvar^2)	ω_3	(USD/Mvar)
	0.30		-305.10		127,380

For comparison, the optimization algorithms reported by the authors of [49] are used to validate the efficiency of the proposed GNDO approach for installing D-STATCOMs in distribution grids. These are the genetic algorithm combined with a particle swarm optimizer (GA/PSO), the vortex search algorithm (VSA), and two solvers available in the GAMS software: COUENNE and BONMIN. Table 8 lists the comparative results for the proposed GNDO approach and the literature reports regarding the optimal location and sizing of D-STATCOMs in distribution grids.

Table 8. Comparative results regarding D-STATCOM location and sizing in the IEEE 33- and 69-bus grids.

IEEE 33-bus Grid					
Method	**Location**	**Size (Mvar)**	z_{cost} **(USD/year)**	**Reduction (%)**	**Time (s)**
Benchmark case	-	-	112,740.90	-	-
COUENNE	[16, 17, 18]	[0.0109, 0.0224, 0.2065]	107,589.50	4.56	3.03
BONMIN	[17, 18, 30]	[0.0339, 0.0227, 0.2395]	102,447.29	9.13	7.59
GA/PSO	[14, 30, 31]	[0.1599, 0.3497, 0.1117]	98,511.63	12.62	6417.91
VSA	[14, 30, 32]	[0.1599, 0.3591, 0.1072]	98,497.90	12.63	59.64
GNDO	[14, 30, 32]	[0.1599, 0.3591, 0.1072]	98,497.90	12.63	47.71
IEEE 69-bus Grid					
Method	**Location**	**Size (Mvar)**	z_{cost} **(USD/year)**	**Reduction (%)**	**Time (s)**
Benchmark case	-	-	119,715.63	-	-
GA/PSO	[21, 61, 64]	[0.0839, 0.4600, 0.1139]	102,990.79	13.97	9325.89
VSA	[21, 61, 64]	[0.0839, 0.4601, 0.1139]	102,990.79	13.97	202.66
GNDO	[21, 61, 64]	[0.0839, 0.4601, 0.1139]	102,990.79	13.97	171.15

The numerical results in Table 8 show that:

i. The proposed GNDO and the VSA approaches reach the exact solution value for the D-STATCOMs in both test feeders, with a final objective function value of about USD 98,497.90 for the IEEE 33-bus grid and USD 102,990.79 in the case of the IEEE 69-bus grid. On the other hand, the GA/PSO approach fails to find the optimal solution in the case of the IEEE 33-bus grid, with an additional investment of about USD 13.73. In contrast, for the IEEE 69-bus grid, the exact solution value is found by the GNDO and the VSA approaches.

ii. The GAMS solvers confirm the nonlinearity and non-convexity of the exact MINLP model, and both solvers are stuck in locally optimal solutions for the IEEE 33-bus grid. The COUENNE solver finds a reduction of about 3.03% in the annual grid operating costs with respect to the benchmark case, while the BONMIN solver reaches a reduction of approximately 7.59%. However, the main problem with these MINLP solvers is that they did not find a feasible solution for the optimal placement and sizing of D-STATCOMs in the IEEE 69-bus grid simulation scenario.

iii. The processing times in the IEEE 33- and 69-bus grids with the proposed GNDO approach showed that, even though it has the same numerical behavior as the VSA, it reports better average processing times, being 11.93 s faster in the IEEE 33 bus grid and 31.51 s faster in the IEEE 69-bus grid. However, it is important to mention that both methods take less than 4 min to locate and size D-STATCOMs in radial distribution networks, whereas the GA/PSO approach takes more than 100 min in both cases. These long simulation times are associated with the fact that the GA selects the nodes where the D-STATCOMS must be located, while the PSO approach determines their optimal sizes. At the same time, the GNDO and VSA methodologies solve both problems using a continuous-discrete codification that allows for drastically reducing the required power flow solutions.

After locating and sizing D-STATCOMs in the IEEE 33- and 69-bus grids, the proposed GNDO approach confirmed its robustness and efficiency in solving problems regarding reactive power compensation in distribution networks, with notable numerical performance when compared to recent literature developments.

5.3.4. Optimal Location of Fixed-Step Capacitor Banks in the IEEE 85-bus Grid

The IEEE 85-bus grid is a medium-voltage distribution network with a radial configuration, operated with 11 kV in the substation located at bus 1. The electrical topology of this test feeder is depicted in Figure 6, and its electrical parameters are listed in Table 9.

Table 9. Parametric information regarding branches and loads in the IEEE 85-bus system.

k	m	R_{km} (Ω)	x_{km} (Ω)	P_k (kW)	Q_k (kW)	k	m	R_{km} (Ω)	x_{km} (Ω)	P_k (kW)	Q_k (kW)
1	2	0.108	0.075	0	0	34	44	1.002	0.416	35.28	35.99
2	3	0.163	0.112	0	0	44	45	0.911	0.378	35.28	35.99
3	4	0.217	0.149	56	57.13	45	46	0.911	0.378	35.28	35.99
4	5	0.108	0.074	0	0	46	47	0.546	0.226	14	14.28
5	6	0.435	0.298	35.28	35.99	35	48	0.637	0.264	0	0
6	7	0.272	0.186	0	0	48	49	0.182	0.075	0	0
7	8	1.197	0.820	35.28	35.99	49	50	0.364	0.151	36.28	37.01
8	9	0.108	0.074	0	0	50	51	0.455	0.189	56	57.13
9	10	0.598	0.410	0	0	48	52	1.366	0.567	0	0
10	11	0.544	0.373	56	57.13	52	53	0.455	0.189	35.28	35.99
11	12	0.544	0.373	0	0	53	54	0.546	0.226	56	57.13
12	13	0.598	0.410	0	0	52	55	0.546	0.226	56	57.13
13	14	0.272	0.186	35.28	35.99	49	56	0.546	0.226	14	14.28
14	15	0.326	0.223	35.28	35.99	9	57	0.273	0.113	56	57.13
2	16	0.728	0.302	35.28	35.99	57	58	0.819	0.340	0	0
3	17	0.455	0.189	112	114.26	58	59	0.182	0.075	56	57.13
5	18	0.820	0.340	56	57.13	58	60	0.546	0.226	56	57.13
18	19	0.637	0.264	56	57.13	60	61	0.728	0.302	56	57.13
19	20	0.455	0.189	35.28	35.99	61	62	1.002	0.415	56	57.13
20	21	0.819	0.340	35.28	35.99	60	63	0.182	0.075	14	14.28
21	22	1.548	0.642	35.28	35.99	63	64	0.728	0.302	0	0
19	23	0.182	0.075	56	57.13	64	65	0.182	0.075	0	0
7	24	0.910	0.378	35.28	35.99	65	66	0.182	0.075	56	57.13
8	25	0.455	0.189	35.28	35.99	64	67	0.455	0.189	0	0
25	26	0.364	0.151	56	57.13	67	68	0.910	0.378	0	0
26	27	0.546	0.226	0	0	68	69	1.092	0.453	56	57.13
27	28	0.273	0.113	56	57.13	69	70	0.455	0.189	0	0
28	29	0.546	0.226	0	0	70	71	0.546	0.226	35.28	35.99
29	30	0.546	0.226	35.28	35.99	67	72	0.182	0.075	56	57.13
30	31	0.273	0.113	35.28	35.99	68	73	1.184	0.491	0	0
31	32	0.182	0.075	0	0	73	74	0.273	0.113	56	57.13
32	33	0.182	0.075	14	14.28	73	75	1.002	0.416	35.28	35.99
33	34	0.819	0.340	0	0	70	76	0.546	0.226	56	57.13
34	35	0.637	0.264	0	0	65	77	0.091	0.037	14	14.28
35	36	0.182	0.075	35.28	35.99	10	78	0.637	0.264	56	57.13
26	37	0.364	0.151	56	57.13	67	79	0.546	0.226	35.28	35.99
27	38	1.002	0.416	56	57.13	12	80	0.728	0.302	56	57.13
29	39	0.546	0.226	56	57.13	80	81	0.364	0.151	0	0
32	40	0.455	0.189	35.28	35.99	81	82	0.091	0.037	56	57.13
40	41	1.002	0.416	0	0	81	83	1.092	0.453	35.28	35.99
41	42	0.273	0.113	35.28	35.99	83	84	1.002	0.416	14	14.28
41	43	0.455	0.189	35.28	35.99	13	85	0.819	0.340	35.28	35.99

Table 10 presents the numerical simulations for the IEEE 85-bus grid, considering the possibility of selecting zero to six nodes with shunt capacitors. In this simulation, each node selected to locate a reactive power compensator must have at least one pack of capacitors installed.

Table 10. Numerical results for the IEEE 85-bus regarding the optimal selection and location of fixed-step capacitor banks.

No. of Nodes	Location	Size (kvar)	f_{NPV} (USD)	Ave. Time (s)
0	—	—	643,005.2405	—
1	26	900	503,325.5728	231.6172
2	[32, 60]	[500, 500]	469,918.4905	360.2201
3	[12, 34, 60]	[200, 400, 400]	463,494.7688	417.9952
4	[12, 35, 40, 64]	[200, 200, 200, 400]	463,290.0220	367.9361
5	[12, 29, 48 60, 68]	[200, 300, 200 200, 200]	461,133.6344	360.5564
6	[27, 35, 53 60, 70, 80]	[200, 300, 100 200, 100, 200]	462,226.7173	471.7108
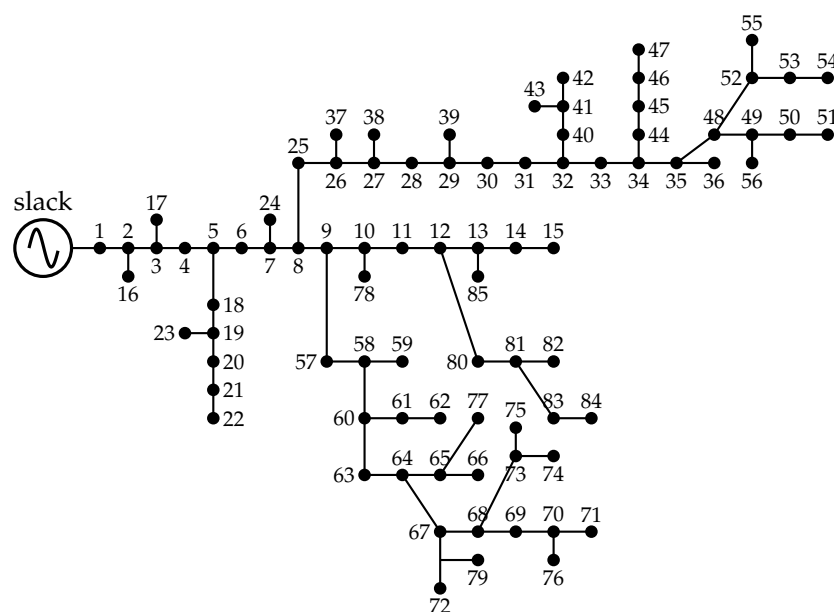
Figure 6. Schematic nodal connections of the IEEE 85-bus grid.

The numerical results in Table 10 reveal that:

i. The maximum reduction in the expected net present value (NPV) is reached when five capacitor banks are installed in the distribution network. These are installed at nodes 12 (200 kvar), 29 (300 kvar), 48 (200 kvar), 60 (200 kvar), and 68 (200 kvar), which summarizes a total of 100 kvar of reactive power injection in the IEEE 85-bus grid, and thus allows for a reduction of about 28.2846%, i.e., USD 181,871.6061.

ii. Solutions containing three and four capacitors show a similar reduction in the expected NPV, both installing 1000 kvar in the form of fixed-step capacitor bank compensators. For three capacitors, these were installed at nodes 12 (200 kvar), 34 (400 kvar), and 60 (400 kvar), which allowed for a reduction of about 27.9174% in the objective function value with respect to the benchmark case. In the case involving four capacitors, these were assigned to nodes 12 (200 kvar), 35 (200 kvar), 40 (200 kvar), and 64 (400 kvar), which allowed for a reduction in the objective function value of about 27.9493% with respect to the benchmark case.

iii. Solutions involving six shunt capacitor banks show that, for the IEEE 85-bus grid, the objective function tends towards saturation after five capacitors, given that, with six devices, the objective function starts to increase again. The reduction with six capacitors was about 28.1146% with respect to the benchmark case (i.e., USD 1093.0829), which is more expensive than the best solution found with five fixed-step capacitor banks. This is a significant result, as it shows that, for the IEEE 85-bus grid, after three shunt capacitors, the expected reduction in the NPV varies by less than 1%, which implies that the distribution company has a variety of reactive power compensa-

tion options to improve their NPV with similar reductions, i.e., between 27.9174% and 28.2846%.

Regarding processing times, it is worth mentioning that implementing the GNDO approach took between 231.6172 s and 471.7108 s to solve the studied problem. This is a reduced processing time considering that only the solution space associated with the nodal selection varies from 84 (for one capacitor package) to 406,481,544 (for six capacitor packages) possible nodal options. In addition, the number of capacitor options per node varies from 10 (for one capacitor package) to 1,000,000 (for six capacitor packages), which implies that the dimensions of the integer part of the MINLP model change from a few hundred to trillions of options.

6. Conclusions and Future Work

The problem regarding the optimal placement and sizing of fixed-step capacitor banks in radial and meshed distribution networks was addressed in this study by applying a master–slave optimization technique. The master stage defined the nodes and the sizes of the fixed-step capacitor banks to be installed, employing the discrete version of the GNDO approach. This discrete configuration determines the purchasing, installing, and operating costs of the fixed-step capacitor banks. The slave stage evaluated each capacitor configuration provided by the master stage in order to determine the expected costs of the energy losses for the planning period. Numerical results in the IEEE 33-bus grid with radial and meshed configurations demonstrated that:

i. For the radial configuration, the best solution reached by the proposed optimization approach involves two packs of capacitor banks at nodes 13 and 30 with sizes of 200, and 500 kvar, allowing for a reduction of about USD 64,937.8319 with respect to the benchmark case, i.e., a net improvement of about 13.8534%. When the optimal solution (two capacitor banks) was compared with the solution involving five capacitor banks, a deterioration of about 0.8412% was observed in the objective function, which confirmed that the increase in number of fixed-step capacitor banks installed did not necessarily improve the expected net present value of the project.

ii. In the case of the meshed configuration for the IEEE 33-bus grid, for only one set of capacitor banks installed at node 30, with an equivalent size of 600 kvar, the best reduction in the objective function value was found, i.e., 7.6881%. However, when the system was forced to install five sets of capacitors, the objective function was deteriorated by about 1.5869% with respect to the optimal solution. This confirmed that each distribution network topology could have a different number of capacitor banks which will allow for a better minimization of the objective function.

iii. Regarding processing times, it was observed that, for the radial simulation, less than 69 s were needed to solve the studied problem with a different number of capacitor banks, whereas, in the meshed configuration, less than 48 s were required. The difference between both processing times is mainly attributable to the fact that, in radial configurations, more iterations are required to ensure the power flow convergence. This is in comparison with a meshed grid structure.

A comparative analysis between the proposed master–slave approach with combinatorial and exact optimization methods in the IEEE 69-bus grid with a radial configuration and peak load conditions confirmed that the GNDO algorithm is an efficient combinatorial optimization method supported by normal distributions to solve hard MINLP models, which opens the possibility of its extension to multiple engineering problems.

Numerical simulations employing the proposed GNDO approach to locate and size D-STATCOMs in the IEEE 33- and 69-bus grids with a radial structure confirmed the effectiveness of this algorithm compared to the GA/PSO and the VSA approaches, where less processing times were required. The exact solution of the VSA approach was found by the GNDO approach in both test feeders. In contrast, the GA/PSO approach, as well as the COUENNE and BONMIN solvers of the GAMS software, exhibited a locally optimal convergence in the IEEE 33-bus grid.

The application of the proposed master–slave approach to locate and select fixed-step capacitor banks in the IEEE 85-bus grid showed that, after three reactive power compensators were installed, the objective function was reduced by less than 1%. The best solution was found when five capacitors were installed, allowing for a reduction of about 28.2846% with respect to the benchmark case. In addition, the solution with six reactive power compensators showed that the objective function started to deteriorate, which confirmed that the best number of shunt capacitor banks for installation is five. However, due to the large dimensions of the solution space, more research will be required to confirm or disprove these results for the IEEE 85-bus grid.

Future works derived from this research could include the following: (i) a sensitivity analysis regarding the interest rates applied to the investment returns, energy losses, and operation costs, as well as with respect to capacitor bank sizes, allowing to find better solutions for each distribution network under analysis; (ii) the inclusion of uncertainties in the demand behavior, as well as the distinction between residential, industrial, and commercial users in the studied problem, by transforming the exact MINLP model into a mixed-integer convex model; and (iii) the combination between reactive power compensators with fixed and variable injection characteristics and active power compensators, i.e., dispersed generation for planning and operation studies in distribution networks that involve the GNDO approach.

Author Contributions: Conceptualization, methodology, software, and writing (review and editing): O.D.M., W.G.-G. and J.C.H. All authors have read and agreed to the published version of the manuscript.

Data Availability Statement: No new data were created or analyzed in this study. Data sharing does not apply to this article.

Conflicts of Interest: The authors declare no conflict of interest.

References

1. Anilkumar, R.; Devriese, G.; Srivastava, A.K. Voltage and reactive power control to maximize the energy savings in power distribution system with wind energy. *IEEE Trans. Ind. Appl.* **2017**, *54*, 656–664. [CrossRef]
2. Prakash, D.B.; Lakshminarayana, C. Optimal siting of capacitors in radial distribution network using whale optimization algorithm. *Alex. Eng. J.* **2017**, *56*, 499–509. [CrossRef]
3. Gil-González, W. Optimal Placement and Sizing of D-STATCOMs in Electrical Distribution Networks Using a Stochastic Mixed-Integer Convex Model. *Electronics* **2023**, *12*, 1565. [CrossRef]
4. El M.A.; Abdel-Gwaad, A.F.; Farahat, M.A. Solving the capacitor placement problem in radial distribution networks. *Results Eng.* **2023**, *17*, 100870.
5. Gil-González, W.; Montoya, O.D.; Grisales-Noreña, L.F.; Trujillo, C.L.; Giral-Ramírez, D.A. A mixed-integer second-order cone model for optimal siting and sizing of dynamic reactive power compensators in distribution grids. *Results Eng.* **2022**, *15*, 100475. [CrossRef]
6. Ali, A.; Abbas, G.; Keerio, M.U.; Mirsaeidi, S.; Alshahr, S.; Alshahir, A. Multi-objective Optimal Siting and Sizing of Distributed Generators and Shunt Capacitors Considering the Effect of Voltage-dependent Nonlinear Load Models. *IEEE Access* **2023**, *11*, 21465–21487. [CrossRef]
7. Gil-González, W.; Montoya, O.D.; Rajagopalan, A.; Grisales-Noreña, L.F.; Hernández, J.C. Optimal selection and location of fixed-step capacitor banks in distribution networks using a discrete version of the vortex search algorithm. *Energies* **2020**, *13*, 4914. [CrossRef]
8. Parashar, S.M.; Leena, G.; Pande, M.; Singh, J. Dynamic Capacitor Placement To Mitigate Disaster in Distribution System: A Fuzzy Approach. In Proceedings of the 2019 International Conference on Power Electronics, Control and Automation (ICPECA), New Delhi, India, 16–17 November 2019; pp. 1–5.

9. Szultka, A.; Małkowski, R. Selection of optimal location and rated power of capacitor banks in distribution network using genetic algorithm. In Proceedings of the 2017 18th International Scientific Conference on Electric Power Engineering (EPE), Kouty nad Desnou, Czech Republic, 17–19 May 2017; pp. 1–6.

10. Soma, G.G. Optimal sizing and placement of capacitor banks in distribution networks using a genetic algorithm. *Electricity* **2021**, *2*, 187–204. [CrossRef]

11. Abou El-Ela, A.A.; El-Sehiemy, R.A.; Kinawy, A.M.; Mouwafi, M.T. Optimal capacitor placement in distribution systems for power loss reduction and voltage profile improvement. *IET Gener. Transm. Distrib.* **2016**, *10*, 1209–1221. [CrossRef]

12. Dehghani, M.; Montazeri, Z.; Dhiman, G.; Malik, O.; Morales-Menendez, R.; Ramirez-Mendoza, R.A.; Dehghani, A.; Guerrero, J.M.; Parra-Arroyo, L. A spring search algorithm applied to engineering optimization problems. *Appl. Sci.* **2020**, *10*, 6173. [CrossRef]

13. Lee, C.S.; Ayala, H.V.H.; dos Santos Coelho, L. Capacitor placement of distribution systems using particle swarm optimization approaches. *Int. J. Electr. Power Energy Syst.* **2015**, *64*, 839–851. [CrossRef]

14. Cao, B.; Li, W.; Zhao, J.; Yang, S.; Kang, X.; Ling, Y.; Lv, Z. Spark-based parallel cooperative co-evolution particle swarm optimization algorithm. In Proceedings of the 2016 IEEE International Conference on Web Services (ICWS), San Francisco, CA, USA, 27 June–2 July 2016; pp. 570–577.

15. Riaño, F.E.; Cruz, J.F.; Montoya, O.D.; Chamorro, H.R.; Alvarado-Barrios, L. Reduction of losses and operating costs in distribution networks using a genetic algorithm and mathematical optimization. *Electronics* **2021**, *10*, 419. [CrossRef]

16. Pérez-Abril, I. Capacitors placement in distribution systems with nonlinear load by using the variables' inclusion and interchange algorithm. *Dyna* **2021**, *88*, 13–22. [CrossRef]

17. Šarić, M.; Hivziefendić, J. Optimal Capacitor Placement in Distribution Network for Loss Reduction and Voltage Profile Improvement. In Proceedings of the 2019 18th International Symposium INFOTEH-JAHORINA (INFOTEH), East Sarajevo, Bosnia and Herzegovina, 20–22 March 2019; pp. 1–4.

18. Asadi, M.; Shokouhandeh, H.; Rahmani, F.; Hamzehnia, S.M.; Harikandeh, M.N.; Lamouki, H.G.; Asghari, F. Optimal placement and sizing of capacitor banks in harmonic polluted distribution network. In Proceedings of the 2021 IEEE Texas Power and Energy Conference (TPEC), Virtually, 2–5 February 2021; pp. 1–6.

19. Esmaeilian, H.R.; Fadaeinedjad, R. Distribution system efficiency improvement using network reconfiguration and capacitor allocation. *Int. J. Electr. Power Energy Syst.* **2015**, *64*, 457–468. [CrossRef]

20. Sedighizadeh, M.; Bakhtiary, R. Optimal multi-objective reconfiguration and capacitor placement of distribution systems with the Hybrid Big Bang–Big Crunch algorithm in the fuzzy framework. *Ain Shams Eng. J.* **2016**, *7*, 113–129. [CrossRef]

21. Montoya, O.D.; Moya, F.D.; Rajagopalan, A. Annual Operating Costs Minimization in Electrical Distribution Networks via the Optimal Selection and Location of Fixed-Step Capacitor Banks Using a Hybrid Mathematical Formulation. *Mathematics* **2022**, *10*, 1600. [CrossRef]

22. Montoya, O.D.; Gil-González, W.; Garcés, A. On the Conic Convex Approximation to Locate and Size Fixed-Step Capacitor Banks in Distribution Networks. *Computation* **2022**, *10*, 32. [CrossRef]

23. Liu, B.J.; Bi, X.J. Adaptive ε-constraint multi-objective evolutionary algorithm based on decomposition and differential evolution. *IEEE Access* **2021**, *9*, 17596–17609. [CrossRef]

24. Huang, T.L.; Hsiao, Y.T.; Chang, C.H.; Jiang, J.A. Optimal placement of capacitors in distribution systems using an immune multi-objective algorithm. *Int. J. Electr. Power Energy Syst.* **2008**, *30*, 184–192. [CrossRef]

25. Rajendran, A.; Narayanan, K. Multi-Objective Hybrid WIPSO–GSA Algorithm-Based DG and Capacitor Planning for Reduction of Power Loss and Voltage Deviation in Distribution System. *Smart Sci.* **2018**, *6*, 295–307. [CrossRef]

26. Shaheen, A.M.; El-Sehiemy, R.A. A multiobjective salp optimization algorithm for techno-economic-based performance enhancement of distribution networks. *IEEE Syst. J.* **2020**, *15*, 1458–1466. [CrossRef]

27. Elshahed, M.; Tolba, M.A.; El-Rifaie, A.M.; Ginidi, A.; Shaheen, A.; Mohamed, S.A. An Artificial Rabbits' Optimization to Allocate PVSTATCOM for Ancillary Service Provision in Distribution Systems. *Mathematics* **2023**, *11*, 339. [CrossRef]

28. Shaheen, A.M.; El-Sehiemy, R.A.; Ginidi, A.; Elsayed, A.M.; Al-Gahtani, S.F. Optimal Allocation of PV-STATCOM Devices in Distribution Systems for Energy Losses Minimization and Voltage Profile Improvement via Hunter-Prey-Based Algorithm. *Energies* **2023**, *16*, 2790. [CrossRef]

29. Montoya, O.D.; Gil-González, W.; Hernández, J.C. Efficient operative cost reduction in distribution grids considering the optimal placement and sizing of D-STATCOMs using a discrete-continuous VSA. *Appl. Sci.* **2021**, *11*, 2175. [CrossRef]

30. Castiblanco-Pérez, C.M.; Toro-Rodríguez, D.E.; Montoya, O.D.; Giral-Ramírez, D.A. Optimal Placement and sizing of D-STATCOM in radial and meshed distribution networks using a discrete-continuous version of the genetic algorithm. *Electronics* **2021**, *10*, 1452. [CrossRef]

31. Ghiasi, M.; Olamaei, J. Optimal capacitor placement to minimizing cost and power loss in Tehran metro power distribution system using ETAP (A case study). *Complexity* **2016**, *21*, 483–493. [CrossRef]

32. Yuan, Z.; Hesamzadeh, M.R. Second-order cone AC optimal power flow: Convex relaxations and feasible solutions. *J. Mod. Power Syst. Clean Energy* **2018**, *7*, 268–280. [CrossRef]

33. Kaur, S.; Kumbhar, G.; Sharma, J. A MINLP technique for optimal placement of multiple DG units in distribution systems. *Int. J. Electr. Power Energy Syst.* **2014**, *63*, 609–617. [CrossRef]

34. Kumar, A.; Gao, W. Optimal distributed generation location using mixed integer non-linear programming in hybrid electricity markets. *IET Gener. Transm. Distrib.* **2010**, *4*, 281. [CrossRef]

35. Bai, X.; Wei, H. A semidefinite programming method with graph partitioning technique for optimal power flow problems. *Int. J. Electr. Power Energy Syst.* **2011**, *33*, 1309–1314. [CrossRef]

36. De Oliveira-De Jesus, P.M.; Alvarez, M.; Yusta, J. Distribution power flow method based on a real quasi-symmetric matrix. *Electr. Power Syst. Res.* **2013**, *95*, 148–159. [CrossRef]

37. Montoya, O.D.; Gil-González, W. On the numerical analysis based on successive approximations for power flow problems in AC distribution systems. *Electr. Power Syst. Res.* **2020**, *187*, 106454. [CrossRef]

38. Garcés-Ruiz, A. Power Flow in Unbalanced Three-Phase Power Distribution Networks Using Matlab: Theory, analysis, and quasi-dynamic simulation. *Ingeniería* **2022**, *27*, e19252. [CrossRef]

39. Montoya, O.D.; Molina-Cabrera, A.; Hernández, J.C. A Comparative Study on Power Flow Methods Applied to AC Distribution Networks with Single-Phase Representation. *Electronics* **2021**, *10*, 2573. [CrossRef]

40. Zhang, Y.; Jin, Z.; Mirjalili, S. Generalized normal distribution optimization and its applications in parameter extraction of photovoltaic models. *Energy Convers. Manag.* **2020**, *224*, 113301. [CrossRef]

41. Vega-Forero, J.A.; Ramos-Castellanos, J.S.; Montoya, O.D. Application of the Generalized Normal Distribution Optimization Algorithm to the Optimal Selection of Conductors in Three-Phase Asymmetric Distribution Networks. *Energies* **2023**, *16*, 1311. [CrossRef]

42. Abdel-Basset, M.; Mohamed, R.; Abouhawwash, M.; Chang, V.; Askar, S. A Local Search-Based Generalized Normal Distribution Algorithm for Permutation Flow Shop Scheduling. *Appl. Sci.* **2021**, *11*, 4837. [CrossRef]

43. Saib, B.; Abdessemed, M.R.; Hocin, R.; Khoualdi, K. Study of Exploration and Exploitation Mechanisms in Nature Inspired Metaheuristics for Global Optimization. In Proceedings of the 12th International Conference on Information Systems and Advanced Technologies "ICISAT 2022", Istanbul, Turkey, 22–23 July 2022; Springer International Publishing: Berlin/Heidelberg, Germany, 2023; pp. 442–453. [CrossRef]

44. Grisales-Noreña, L.F.; Garzón-Rivera, O.D.; Ocampo-Toro, J.A.; Ramos-Paja, C.A.; Rodriguez-Cabal, M.A. Metaheuristic Optimization Methods for Optimal Power Flow Analysis in DC Distribution Networks. *Trans. Energy Syst. Eng. Appl.* **2020**, *1*, 13–31. [CrossRef]

45. Shuaib, Y.M.; Kalavathi, M.S.; Rajan, C.C.A. Optimal capacitor placement in radial distribution system using Gravitational Search Algorithm. *Int. J. Electr. Power Energy Syst.* **2015**, *64*, 384–397. [CrossRef]

46. Abul'Wafa, A.R. Optimal capacitor allocation in radial distribution systems for loss reduction: A two stage method. *Electr. Power Syst. Res.* **2013**, *95*, 168–174. [CrossRef]

47. Sultana, S.; Roy, P.K. Optimal capacitor placement in radial distribution systems using teaching learning based optimization. *Int. J. Electr. Power Energy Syst.* **2014**, *54*, 387–398. [CrossRef]

48. Tamilselvan, V.; Jayabarathi, T.; Raghunathan, T.; Yang, X.S. Optimal capacitor placement in radial distribution systems using flower pollination algorithm. *Alex. Eng. J.* **2018**, *57*, 2775–2786. [CrossRef]

49. Grisales-Noreña, L.F.; Montoya, O.D.; Hernández, J.C.; Ramos-Paja, C.A.; Perea-Moreno, A.J. A Discrete-Continuous PSO for the Optimal Integration of D-STATCOMs into Electrical Distribution Systems by Considering Annual Power Loss and Investment Costs. *Mathematics* **2022**, *10*, 2453. [CrossRef]